

# Effect of Asymmetry on Hemodynamics in Fluid-Structure Interaction Model of Congenital Bicuspid Aortic Valves

Gil Marom, Hee-Sun Kim, Moshe Rosenfeld, Ehud Raanani, and Rami Haj-Ali

**Abstract**— A bicuspid aortic valve (BAV) is a congenital cardiac disorder where the valve consists of only two cusps instead of three in a normal tricuspid valve (TAV). Although 97% of BAVs include asymmetric cusps, little or no prior studies investigated the blood flow through physiological three-dimensional BAV and root. This study presents four fully coupled fluid-structure interaction (FSI) models, including native TAV, asymmetric BAV with or without a raphe and an almost symmetric BAV. The FSI simulations are based on coupled structural and fluid dynamics solvers that allow accurate modeling of the pressure load on both the root and the cusps. The partitioned solver has non-conformal meshes and the flow is modeled employing an Eulerian approach. The cusps tissue in the structural model is composed of hyperelastic finite elements with collagen fiber network embedded in the elastin matrix. The tissues behavior of the aortic sinuses is also hyperelastic. The coaptation is modeled with master-slave contact algorithm. A full cardiac cycle is simulated by imposing the same physiological blood pressure at the upstream and downstream boundaries, for all the TAV and BAV models. The latter have significantly smaller opening area compared to the TAV. Larger stress values were also found in the cusps of the BAV models with fused cusps, both at the systolic and diastolic phases. The asymmetric geometry cause asymmetric vortices and much larger wall shear stress on the cusps, which is a potential cause for early valvular calcification in BAVs.

## I. INTRODUCTION

The bicuspid aortic valve (BAV) is a congenital cardiac disorder where the aortic valve consists of only two cusps instead of three in a normal valve. Although this disorder affects 1 to 2% of the population [1], 45 to 49% of the patients with diagnosed aortic stenosis have a bicuspid valve [2]. Recent studies suggest that hemodynamics is a potential cause of the valvular calcification [3]. Surgical pathology studies demonstrated that 97% of BAVs include asymmetric cusps, where two cusps are fused into a single cusp with a central fibrous raphe [1].

Experimental studies on the mechanics of BAV included in-vitro [4,5] and in-vivo [6] experiments. Most of the existing computational BAV models did not include the influence of the flow and were limited to “dry” finite element

This work was partially supported by a grant from the Nicholas and Elizabeth Slezak Super Center for Cardiac Research and Biomedical Engineering at Tel Aviv University.

Gil Marom, Moshe Rosenfeld and Rami Haj-Ali are with the School of Mechanical Engineering, Tel-Aviv University, Tel Aviv 69978, Israel (e-mail: maromgil@eng.tau.ac.il).

Hee-Sun Kim is with the Department of Architectural Engineering, Ewha Womans University, Seoul 120-750, South Korea

Ehud Raanani is with the Cardiothoracic Surgery Department, Chaim Sheba Medical Center, Tel Hashomer 52621, Israel

analysis [7,8]. Conti et al. [7] compared asymmetric BAV, with or without raphe, and tricuspid aortic valve (TAV) and found that BAV model has higher stresses compared to TAV and that the existence of a raphe reduced stress in its region but increased them in the other cusp. Jermihov et al. [8] modeled five different morphologies, including asymmetric TAV, symmetric BAV and two types of BAVs that have fused cusps with or without raphe. They also found that BAVs have higher stresses than TAVs, but stress distribution in the raphe region of their model was increased.

Few studies modeled the hemodynamics of BAV. Richards et al. [9] modeled the flow through bicuspid mechanical heart valve (BMHV) by assuming axisymmetric and fixed geometry, therefore a computational fluid dynamics (CFD) model was employed. Since the kinematics and dynamics of the aortic valve are highly dependent on the combined mechanical properties of the valve and the blood flow, many of the studies used fluid-structure interaction (FSI) models. However, most of these studies modeled BMHVs with rigid valves [10,11]. Two studies investigated BAV using FSI analysis. Weinberg and Kaazempur Mofrad [12] compared multiscale models of BAV and TAV. The FSI model of the organ scale was simulated with the commercial LS-Dyna code that can simulate compressible flow and an explicit solver. They focused on the hemodynamics, however, their BAV had a rare symmetric geometry, since the simulation included only one quarter or one sixth of the region in the BAV and TAV models, respectively. Chandra et al. [13] investigated the influence of asymmetry in two-dimensional (2D) FSI models of TAV and BAVs with different morphologies. The tissues in their model were assumed isotropic and linear elastic and the model included only the systolic phase. In their hemodynamic analysis, they found larger vortices and abnormal wall-shear stress on BAV cusps.

Although hemodynamics may be the cause for the common BAV calcification, none of the previous studies investigated the influence of the asymmetric BAV configuration on hemodynamics. The aim of the present study is to examine this effect using a full FSI models for several morphologies of BAV and TAV with realistic and physiologic blood pressure and tissues properties.

## II. METHODS

A three-dimensional (3D) geometry of a TAV and root was reconstructed using dimensions and geometric relationships similar to those suggested by Thubrikar [2]. Figure 1 illustrates a proposed valve geometry with dimensions that are scaled with respect to the annulus diameter ( $d_{AA}$ ). The geometry of BAV no.1 was calculated

by fusing two cusps from the TAV geometry, and was used in two models with and without raphe. The geometry of BAV no. 2 was constructed in similar manner to the TAV geometry, but with two asymmetric cusps and sinuses ( $195^\circ$ - $165^\circ$ ) instead of three symmetric cusps ( $120^\circ$  each). Figure 2 compares these four initial geometries. The cusps and the root were assumed to have separate but connected geometries; the cusps moved with the root at their joint boundaries. Two straight rigid tubes were added upstream and downstream, respectively, to move the flow boundary conditions away from the regions of interest.

The structural solver employed an implicit nonlinear dynamic analysis with an implicit direct displacement-based finite element method. The Collagen Fiber Network (CFN) material model [14] was employed for the cusps tissues. The CFN model explicitly recognizes the collagen fibers (marked in Fig. 2) and elastin matrix using different layers of elements. The hyperelastic behavior of the two materials and the radii of the fibers in various regions of the cusp were calibrated to published experimental stress-strain curves from porcine aortic valve [15]. Two models with geometry of BAV no. 1 were considered one without raphe and the other includes raphe (marked in yellow in Fig. 2). The raphe was assumed to have stiffer material relative to the

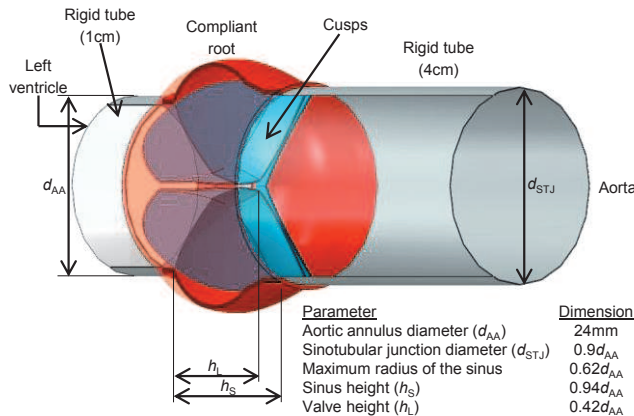


Figure 1. A schematic view of the tricuspid valve model showing the compliant region and the added rigid tubes.

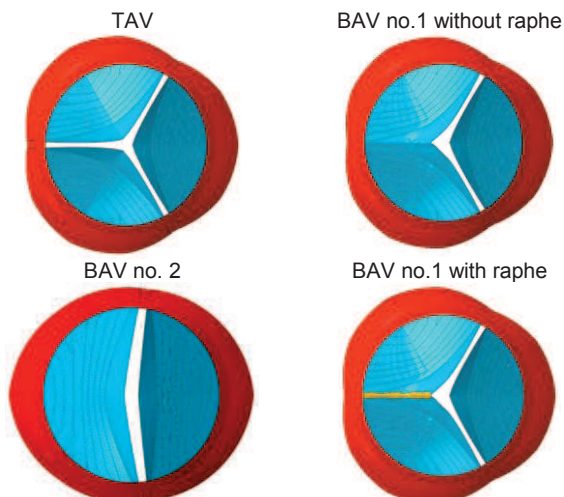


Figure 2. Four types of initial geometries of tricuspid (TAV) and bicuspid (BAV) aortic valves.

surrounding tissue [8]. The tissue of the aortic root was assumed to be isotropic and hyperelastic based on available experimental data of porcine aortic sinuses [16]. A master-slave contact algorithm was employed between the cusps. The mesh of the structural parts in the TAV and BAV no. 1 models have more than 14,000 elements, which was found to be adequate following a mesh refinement study [17]. The structural part of BAV no. 2 was meshed in the same method.

The flow was assumed to be laminar and the blood to be Newtonian and isothermal at temperature of  $37^\circ\text{C}$ . To improve the convergence of the FSI model the blood was assumed to be slightly compressible [17]. A finite volume method was employed for solving the unsteady 3D Navier-Stokes and mass conservation equations using the Eulerian approach with a Cartesian mesh. Physiologic time dependent pressures were employed at the upstream and downstream boundaries, representing the pressures at the left ventricle and the ascending aorta, respectively, as shown in Figure 3. The flow domain was discretized with a mesh of approximately 700,000 elements following a mesh refinement study [17]. The mesh was dynamically adapted in the vicinity of the walls, including near the moving cusps and the compliant root. The implicit flow solver used a spatially second order upwind scheme as well as a second order temporal discretization.

The FSI models were solved by a partitioned solver with non-conformal meshes, which facilitated large structural motion through the fluid domain and simplified the introduction of contact. The sequential two-way coupling process exchanged the structure displacement and velocities, and the calculated traction load (including the fluid pressure and shear) between the solvers. The structural problem was solved by Abaqus 6.10 (Simulia Corp., Providence, RI, USA) finite element software, while FlowVision HPC 3.08 (Capvidia NV, Leuven, Belgium) was the flow solver. FlowVision Multi-Physics manager (Capvidia NV, Leuven, Belgium) managed the coupling of the two codes.

### III. RESULTS

Since this study focuses on the hemodynamics, the four models are compared in the peak systole. For this use, the peak systole is defined as the time when the valve reaches its maximum opening. In the current models, the peak systole was at 80ms and 96ms after the beginning of the opening for the BAV and TAV models, respectively. A possible

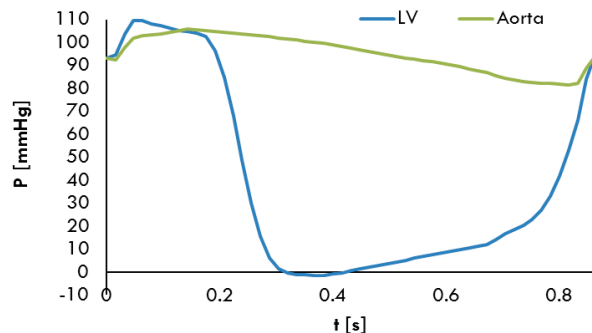


Figure 3. The aortic and left ventricle pressure as a function of time.

explanation is that the TAV has larger opening area and extra time is needed to reach it. The peak systole position is shown in Figure 4 with a plot of the maximum principal stress distribution on the deformed structure. The largest stress is found for the models with BAV no. 1 geometry. Larger stress can be found in the raphe region relative to the

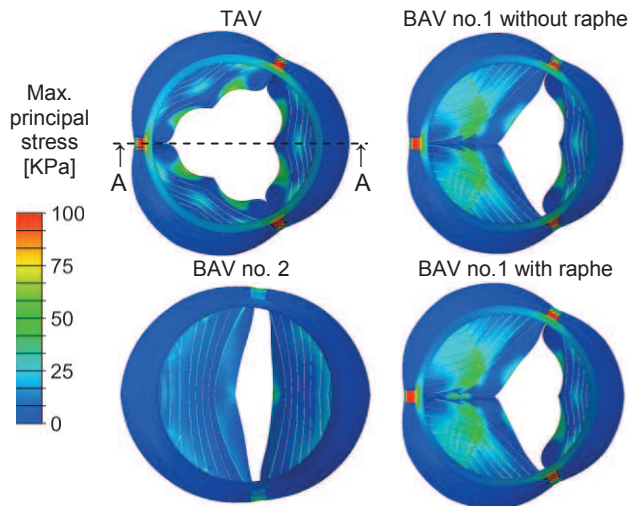


Figure 4. Maximum principal stress distribution on the four types of aortic valves during peak systole.

same region in BAV no. 1 without a raphe, but the difference is not significant. This result is rather different from published in-plane principal stress during peak systole, where much larger stress was found in the raphe region [8]. In general, the largest stress in the cusps is always found in the collagen fibers. Although BAV no. 2 has the smallest stress distribution in the cusps, it is not very efficient because of the very small opening. Those findings are in agreement with published results [8].

Figure 5 presents flow velocity vectors on A-A section (Fig. 4) and the instantaneous streamlines (that are calculated from the instantaneous velocity) at peak systole for the four models. It should be emphasized that although the A-A section is the symmetry plane of all the models, the cusps look asymmetric (Fig. 5) unlike the typical echocardiography view. It is also worth noticing that the flow is 3D and the vortical structure is the same. It can be clearly seen that the asymmetric flow in the BAVs cause large vortices, and the blood reach the aorta at lower velocity than in the TAV model (right boundary of the domain). Similar findings have been reported from in-vitro experiments [5] and from 2D models of asymmetric BAVs [13]. The addition of the raphe causes no noticeable difference. The TAV model has the lowest velocity magnitude near the tissues of the valve and there are no vortices inside the sinuses or near the cusps in this phase of the cardiac cycle. On the other hand, there are

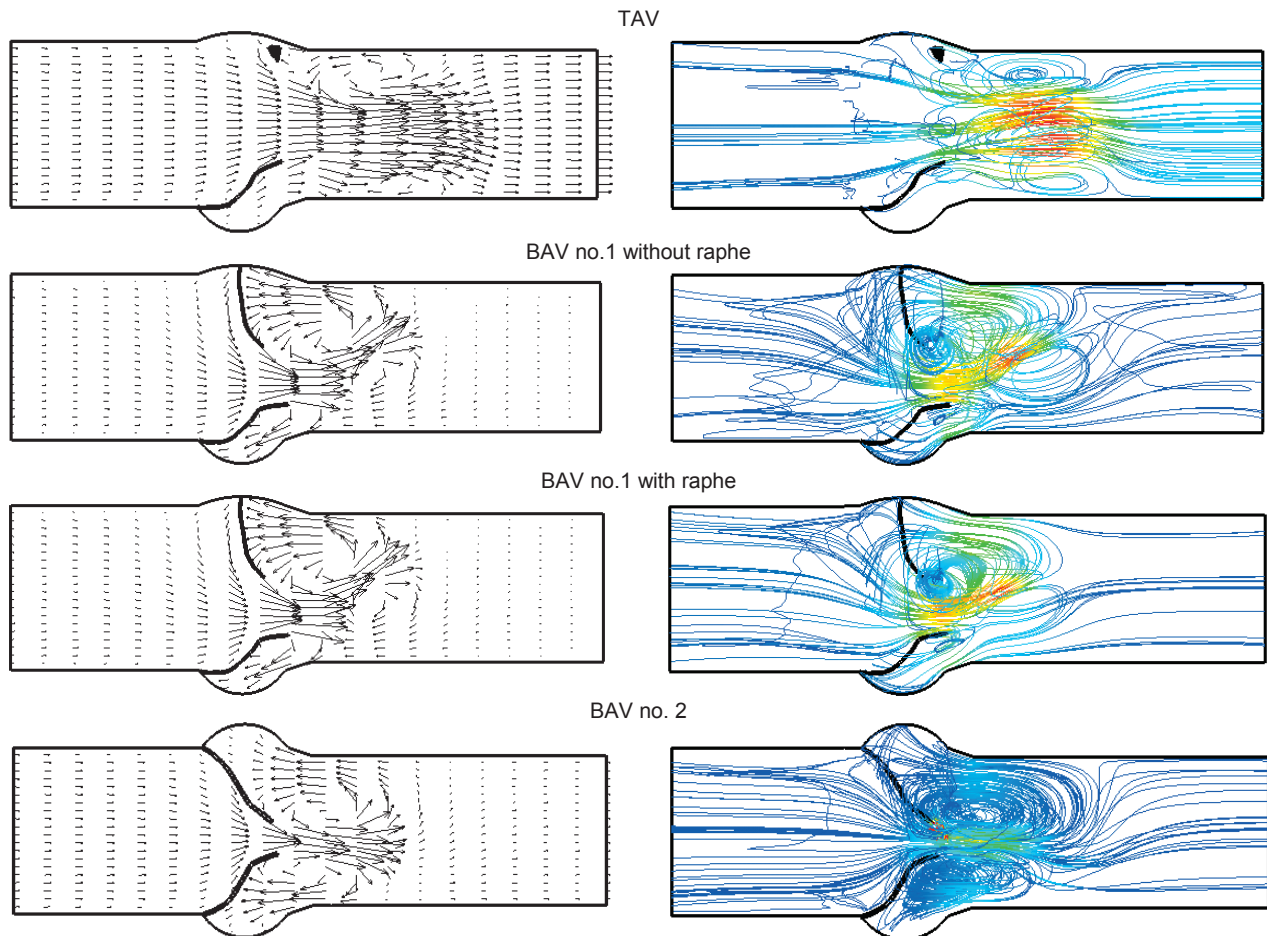


Figure 5. Velocity vectors on A-A section (Fig. 4) and streamlines during peak systole for the four types of aortic valves.

vortices in the sinuses of all the BAV models. The velocity magnitude of these vortices is quite large even near the cusps, especially for the fused cusp in BAV no. 1 models. In all the three BAV models, larger vortices are found in the sinus of the larger cusp.

Figure 6 presents the flow shear stress on the cusps of the four models. For clarity, the root is not shown in Fig. 6 although it was included in all the models. The asymmetric vortices are probably the cause for the larger shear stress that found on the cusps of the BAVs. The TAV model has the lowest shear stress on both sides of the cusps and specifically on the inner side of the coapting regions, because of the lower velocity in this region. The entire aortic side of the fused cusp in BAV no.1 has relatively large shear stress, compared to the TAV model or the smaller cusp in the same model. The belly region of the fused cusp has also larger shear stress relative to the BAV no. 2 with smoother geometry of its cusps. Both sides of the coapting regions in BAV no. 2 have relatively large shear stress. Even though BAV no. 2 is asymmetric, similar shear stress distribution is found on both cusps.

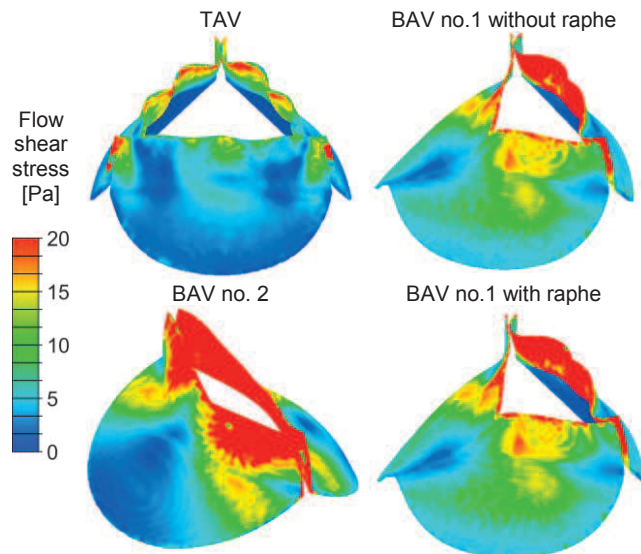


Figure 6. Blood flow shear stress distribution on the four types of aortic valves during peak systole.

#### IV. CONCLUSIONS

Three-dimensional FSI models of TAV and BAVs with compliant root, physiological blood pressure and realistic anisotropic hyperelastic material behavior have been developed. This study focuses on the systolic phase of the cardiac cycle since it investigates mainly the hemodynamics. The results show that in peak systole the stress in the cusps and the flow shear stress on the cusps of BAV with fused cusps are significantly larger than in the TAV model. The combination of large velocity magnitude and asymmetric vortices lead to high flow shear stress magnitudes in the cusps of the BAVs. This is of particular importance since congenital BAV with fused cusps is one of the most common cardiac disorders, with many of its patients also suffering from valvular calcification.

#### REFERENCES

- [1] A. C. Braverman, H. Güven, M. A. Beardslee, M. Mekan, A. M. Kates and M. R. Moon, "The bicuspid aortic valve," *Curr. Probl. Cardiol.*, vol. 30, no. 9, pp. 470 – 522, 2005.
- [2] M. Thubrikar, *The Aortic Valve*. Boca Raton, FL: CRC Press, 1990, pp. 8-15, 158-160.
- [3] K. Balachandran, P. Sucusky and A. P. Yoganathan, "Hemodynamics and mechanobiology of aortic valve inflammation and calcification," *Int. J. Inflamm.*, vol. 2011, DOI:10.4061/2011/263870, 2011.
- [4] F. Robicsek, M. J. Thubrikar, J. W. Cook and B. Fowler, "The congenitally bicuspid aortic valve: how does it function? why does it fail?" *Ann. Thorac. Surg.*, vol. 77, no. 1, pp. 177–185, 2004.
- [5] N. Saikrishnan, C. H. Yap, N. C. Milligan, N. V. Vasilyev and A. P. Yoganathan, "In vitro characterization of bicuspid aortic valve hemodynamics using particle image velocimetry," *Ann. Biomed. Eng.*, DOI:10.1007/s10439-012-0527-2, 2012.
- [6] A. J. Barker, C. Lanning and R. Shandas, "Quantification of hemodynamic wall shear stress in patients with bicuspid aortic valve using phase-contrast MRI," *Ann. Biomed. Eng.*, vol. 38, no. 3, pp. 788–800, 2010.
- [7] C. A. Conti, A. Della Corte, E. Votta, L. Del Viscovo, C. Bancone, L. S. De Santo and A. Redaelli, "Biomechanical implications of the congenital bicuspid aortic valve: a finite element study of aortic root function from in vivo data," *J. Thorac. Cardiovasc. Surg.*, vol. 140, No. 4, pp. 890–896, 2010.
- [8] P. Jermihov, L. Jia, M. S. Sacks, R. Gorman, J. Gorman and K. Chandran, "Effect of geometry on the leaflet stresses in simulated models of congenital bicuspid aortic valves," *Cardiovasc. Eng. Technol.*, vol. 2, no. 1, pp. 48–56, 2011.
- [9] K. E. Richards, D. Deserranno, E. Donal, N. L. Greenberg, J. D. Thomas and M. J. Garcia, "Influence of structural geometry on the severity of bicuspid aortic stenosis," *Am. J. Physiol. Heart Circ. Physiol.*, vol. 287, no.3, pp. H1410–H1416, 2004.
- [10] T. Hong and C. N. Kim, "A numerical analysis of the blood flow around the bileaflet mechanical heart valves with different rotational implantation angles," *J. Hydrodyn. Ser. B*, vol. 23, no. 5, pp. 607 – 614, 2011.
- [11] I. Borazjani, G. Iman and F. Sotiropoulos, "High-resolution fluid–structure interaction simulations of flow through a bi-leaflet mechanical heart valve in an anatomic aorta," *Ann. Biomed. Eng.*, vol. 38, no. 2, pp. 326-344, 2010.
- [12] E. J. Weinberg and M. R. Kaazempur Mofrad, "A multiscale computational comparison of the bicuspid and tricuspid aortic valves in relation to calcific aortic stenosis," *J. Biomech.*, vol. 41, no. 16, pp. 3482–3487, 2008.
- [13] S. Chandra, N. Rajamannan and P. Sucusky, "Computational assessment of bicuspid aortic valve wall-shear stress: implications for calcific aortic valve disease," *Biomech. Model. Mechanobiol.*, DOI:10.1007/s10237-012-0375-x, 2012.
- [14] H. S. Kim, "Nonlinear multi-scale anisotropic material and structural models for prosthetic and native aortic heart valves," PhD thesis, Georgia Institute of Technology, Atlanta, GA, USA, 2009.
- [15] Y. F. Missirlis and M. Chong, "Aortic valve mechanics - part 1: material properties of natural porcine aortic valves," *J. Bioengr.*, vol. 2, no. 3-4, pp. 287-300, 1978.
- [16] N. Gundiah, P. B. Matthews, R. Karimi, A. Azadani, J. Guccione, T. S. Guy, D. Saloner and E. E. Tseng, "Significant material property differences between the porcine ascending aorta and aortic sinuses," *J. Heart Valve Dis.*, vol. 17, no. 6, pp. 606-613, 2008.
- [17] G. Marom, R. Haj-Ali, E. Raanani, H. J. Schäfers and M. Rosenfeld, "A fluid-structure interaction model of coaptation in fully compliant aortic valves," *Med. Biol. Eng. Comput.*, vol. 50, no. 2, pp. 173-182, 2012.